Journal of Engineering, National Chung Hsing University, Vol. 20, No. 3, pp. 161-169 (2009)

DESIGN AND ANALYSIS OF A BEZIER-PROFILE HORN

Dung-An Wang [a,*] Wei-Yang Chuang [b] Kei Hsu [b] Huy-Tuan Pham [a]

[a] *Institute of Precision Engineering,*
National Chung Hsing University,
Taichung 402, Taiwan, R.O.C.
[b] *Precision Machinery Research and Development Center,*
Taichung 407, Taiwan, R.O.C.

Keywords: Bézier curve; Ultrasonic actuation; Displacement amplification.

ABSTRACT

A new horn for high displacement amplification has been designed and tested. The profile of the horn is a cubic Bézier curve. The design of the horn is based on an optimization procedure where the profile of the horn is optimized via the parameters of a cubic Bézier curve to meet the requirement of displacement amplification. Finite element analyses are carried out to obtain accurate modal frequency and displacement solutions for the proposed horn. A horn prototype has been fabricated. Based on the finite element analyses, maximum Mises stress of the proposed horn is much lower than that of the catenoidal horn. Experimental results of the harmonic response of the fabricated horn confirm the effectiveness of the design method. The experimental results show that the Bézier horn has the displacement amplification 50% larger than the catenoidal horn. The proposed horn may be more suitable than the classical stepped and catenoidal horns in application where high displacement amplification and low stress concentration are required.

貝茲曲線變幅桿之設計與分析

王東安 [1,*] 莊維彥 [2] 許朝凱 [2] 范輝尊 [3]

關鍵詞：貝茲曲線、超音波致動、位移放大

[1] 國立中興大學精密工程研究所助理教授
[2] 財團法人精密機械研究發展中心
[3] 國立中興大學精密工程研究所研究生
[*] Corresponding author, E-mail: daw@dragon.nchu.edu.tw

摘 要

本文提出一個新的超音波變幅桿之設計，應用於位移放大之變幅桿的輪廓是一個貝茲曲線。變幅桿之設計是使用一個演化運算法，並搭配有限元素分析進行最佳化設計。本研究以數值加工方式製作所設計之變幅角，對照實驗之頻域分析結果與模擬之結果，驗證了此設計方式的有效性。

1. INTRODUCTION

Ultrasonic horns have been widely used in atomizers [1], ophthalmic surgery [2], welding devices [3], wire bonding [4,5], ultrasonic motor [6], ultrasonic lubrication [7] and ultrasonic bistoury [8]. Different profiles such as Gaussian [9], Fourier, exponential [10], stepped [11,12], sinusoidal [13], conical, catenoidal [14] and spline [15], have been proposed and investigated by many researchers. Salmon [16] synthesized a new family of horns in which the exponential horn is a centrally located member. In comparing with the traditional horns, new horns with non-straight structures may offer higher displacement amplification. Sherrit et al. [17] presented a folded horn in order to reduce the length of the resonator. Iula et al. [18] proposed an ultrasonic horn vibrating in a flexural mode.

Conical, exponential, catenoidal, stepped and Gaussian are the most commonly used horns [19]. Abromov [19] points out that the displacement amplification of catenoidal horns is greater than that of exponential or conical ones and less than that of stepped horns. Gaussian horns may possess high displacement amplification, but numerical methods might be needed for the design of Gaussian horns. Development of new horns is needed in application where very high displacement amplification and simple transducer structure are required.

Parametric curve based geometry is flexible enough to give a much better control over the profile of horns for design purpose. In parametric form each coordinate of a point on a curve is represented as a function of a single parameter [20]. Therefore, it has more potential to find higher displacement amplification while keeping the stress in the horns low. Because the parametric curve has more freedom to define the horn profile, it is a more difficult problem to optimize the performance of the horn. Finite element method (FEM) has been used to study and analyze behaviors of horns [18,21]. Using FEM, detailed stress and displacement distributions can be obtained. Fu et al. [22] discussed the design of a piezoelectric transducer with a stepped horn via multiobjective optimization. They formulated the optimization problem using Pareto-based multiobjective genetic algorithms [22]. In order to design horns with conflicting design objectives, the genetic algorithms capable of finding multiple optimal solutions in a single optimization run may be used.

In this investigation, design and analysis of a new horn for high displacement amplification are presented. The design is based on a cubic Bézier curve. The optimal designs of the horns are sought by a multiobjective optimization algorithm. Prototypes of horns are fabricated and tested. The experimental results are in good agreement with those based on the optimization design procedure.

2. DESIGN

Fig. 1 schematically shows a horn driven by a Langevin transducer. A cylindrical coordinate system

is also shown in the figure. The horn is a displacement amplifier designed to work in a longitudinal mode. The Langevin transducer is composed of a couple of piezoelectric disks poled along z direction but with opposite polarities. Its two steel cylinders have radius identical to that of the disks. The flange allows the mounting of the Langevin transducer at the longitudinal nodes. The horn is actuated by the transducer at the designated frequency. The nearly uniformly distributed displacement of the Langevin transducer is transformed into a longitudinal deformation of the horn. A typical displacement distribution curve in also shown in the figure. By proper design of the horn structure, the longitudinal mode of vibration of the horn can be excited, and a large displacement amplification can be obtained.

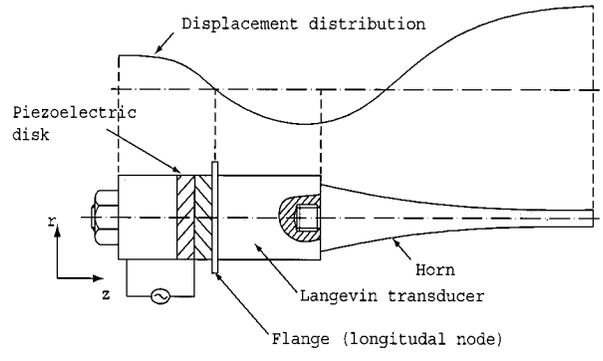

Fig. 1. Schematic of a horn and a Langevin transducer.

The design of the horn for high displacement magnification is based on an optimization procedure where the profile of the horn is optimized via the parameters of a cubic Bézier curve to meet the requirement of displacement amplification. The cubic Bézier curve is determined by a four-point Bézier polygon $Q_0Q_1Q_2Q_3$ as shown in Fig. 2. As described by Rogers and Adams [20], the first and last points, Q_0 and Q_3, respectively, on the curve are coincident with the first and last points of the defining polygon. The tangent vectors at the ends of the curve have the same directions as the first and last polygon spans, respectively. The parametric cubic Bézier curve is given by [20]

$$P(t) = \begin{bmatrix} (1-t)^3 & 3t(1-t)^2 & 3t^2(1-t) & t^3 \end{bmatrix} \begin{bmatrix} P_{Q_0} \\ P_{Q_1} \\ P_{Q_2} \\ P_{Q_3} \end{bmatrix} \quad 0 \le t \le 1 \tag{1}$$

where t is the parameter, and P_{Q_i} is the position vector of the point Q_i.

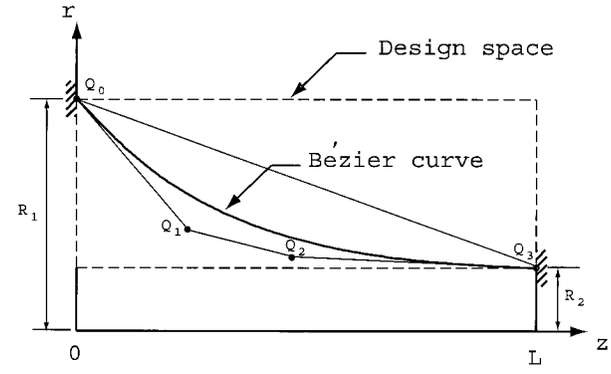

Fig. 2. A profile of a Bézier horn and its four control points Q_0, Q_1, Q_2 and Q_3. The length and radius of the horn are denoted as L and R_1, respectively.

The profile of the horn is optimized by allowing points Q_1 and Q_2 to move in the design space enclosed by the dashed rectangle in Fig. 2. The positions of the points Q_0 and Q_3 are fixed by the specified radius of the back and front end of the horn, R_1 and R_2, respectively, and the length of the horn, L. The horn is assumed to be axisymmetric. An optimization procedure is developed and outlined in Fig. 3. The nondominated sorting genetic algorithm [23] is applied to the optimization of the horn profile. The algorithm is suitable for solving constrained multiobjective problems. The genetic algorithm uses a binary tournament selection and the crowded-comparison operator [23]. In the binary tournament

selection process, two individuals are selected at random and their fitness is compared. The individual with better fitness is selected as a parent. The crowded-comparison operator guides the selection process at the various stages of the algorithm toward a uniformly spread-out Pareto-optimal front [23].

In the optimization process as shown in Fig. 3, initially, the working frequency f and the geometry parameters R_1, R_2 and L are specified. The objective functions of the optimization problem are

$$\begin{aligned} &Min \quad f - f_0 \\ &Max \quad M = \frac{u_{Q_3}}{u_{Q_0}} \end{aligned} \tag{2}$$

where f_0 is the first longitudinal modal frequency of the population of each generation of the horn. M is the amplification of the displacement defined by the ratio of the longitudinal displacement at the front end to that of the back end of the horn. The fast nondominated sorting approach [23] is used to solve the two-objective optimization problem. In the sorting procedure, the concept of Pareto dominance [24] is utilized to evaluate fitness or assigning selection probability to solutions. The population is classified into non-dominated fronts based on its rank in the population, not its actual objective function values.

The proposed horn is designed to have the same working frequency as the Langevin transducer. Due to the geometry complexity, the modal frequency f_0 and the displacement amplification M of the Bézier horn cannot be calculated analytically. Finite element analysis by a commercial software ANSYS is utilized to obtain f_0 and M of the horn.

3. ANALYSIS

3.1 Finite element model

In order to obtain accurate modal frequency and displacement solutions for the proposed horn, finite element analyses are carried out. Fig. 4(a) shows a schematic of the horn with the length L and the diameters D_1 and D_2 of the back and front ends, respectively. A cylindrical coordinate system is also shown in the figure. Due to symmetry, an axisymmetric model of the horn is considered. Fig. 4(b) shows a mesh for an axisymmetric finite element model. The displacement in the r direction of the symmetry axis, the z axis, is constrained. A harmonic displacement in the z direction is applied to the nodes at the back end surface of the horn.

In this investigation, the material of the horn is assumed to be linearly elastic. The Young's modulus and Poisson's ratio are taken as 210 GPa and 0.3, respectively. The density is taken as 7800 Kg/m^3. The commercial finite element program ANSYS is employed to perform the computations. 8-node quadratic element PLANE82 is used to model the horn.

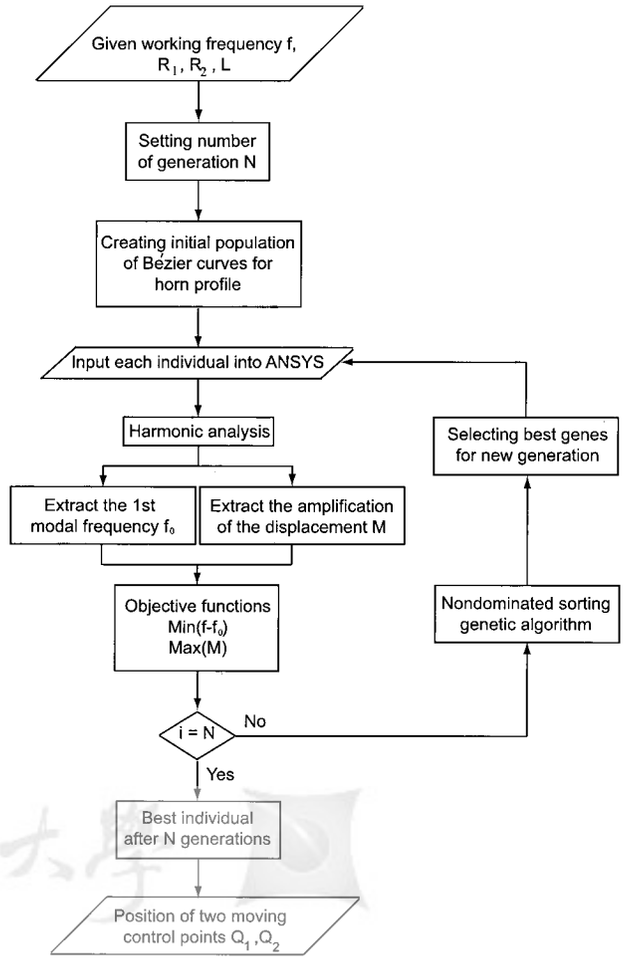

Fig. 3. Flowchart of the optimization procedure.

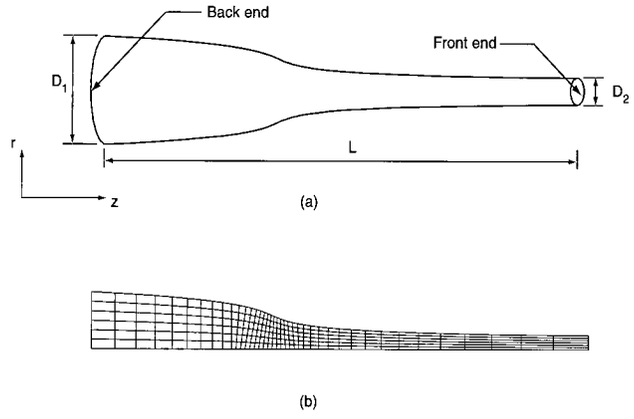

Fig. 4. (a) Schematic of the horn with the length L and the diameters D_1 and D_2 of the back and front ends, respectively. (b) A mesh for an axisymmetric finite element model.

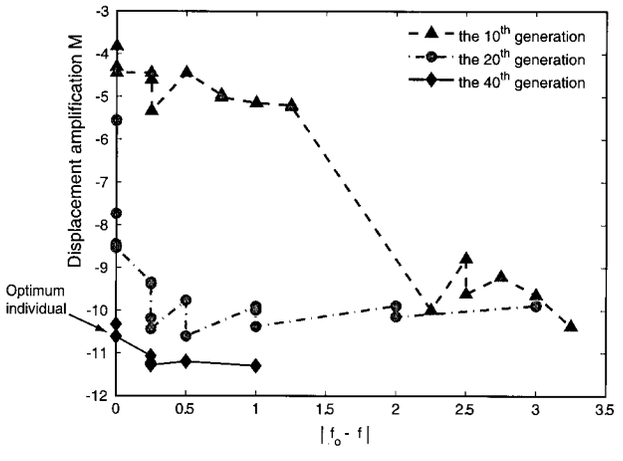

Fig. 5. Distribution of the population of several generations in the optimization process.

3.2 Numerical analysis

In the optimization process, the number of generations, N, is set to be 40, and the population of each generation is taken as 20. The length L and the diameters D_1 and D_2 of the back and front end of the horn are specified as 93 mm, 20 mm and 5 mm, respectively. The working frequency f is set to be 27.9 kHz. In the experiments, the fabricated horn is driven by a Langevin transducer. The available commercial Langevin transducer is purchased from a local vendor. The working frequency of the Langevin transducer is a known and fixed parameter. The Bézier horn is designed to have its first modal frequency equal to the working frequency of the transducer. Therefore, we only consider the horn in the optimization process. Indeed, the modal frequency of the structure including transducer, flange and the horn should be different from that of the horn alone. In this investigation, we concentrate on the design of the new horn. In order to obtain better performance of the horn, its working frequency should be taken as the modal frequency of the whole structure including its driving unit and the flange.

A modal analysis of each population is performed in order to find its first modal frequency f_0 and displacement amplification M. The harmonic response during the optimization process shows that the front end of the horn has its maximum displacement at 27.9 kHz. The displacement amplification is determined by the ratio of the displacement peaks of the harmonic response. Fig. 5 shows the distribution of the population of several generations in the optimization process. The abscissa represents the difference between f and f_0. The ordinate represents the displacement amplification. The displacement amplification is increased dramatically after 40 generations. As also shown in Fig. 5, the difference between f and f_0 of the best of the population in each generation is nearly zero. Fig. 6(a) shows the profile of an optimized Bézier horn. The position of its control points are also shown in the figure.

In order to compare the performances of the proposed horn with classical horns, a catenoidal horn and a stepped horn are also modeled. The stepped horn has the largest displacement amplification among the commonly used horns. However, its high stress occurring near the abruptly changing section is not favored. The catenoidal horn has smaller displacement amplification and a smoother stress distribution than the stepped horn. The new horn discussed in this paper may have larger displacement amplification than the catenoidal horn, and lower stress concentration than the

stepped horn. Here, the stepped, catenoidal and Bézier horns are selected based on the criteria of displacement amplification and Mises stress.

For fair comparison, the catenoidal horn has the same back and front end radiuses and length as those of the proposed horn. The working frequency of the catenoidal horn obtained by a finite element analysis is 28.3 kHz. The back and front end radiuses of the stepped horn are the same as those of the proposed horn. In order to have the same working frequency of 27.9 kHz as the proposed horn, the length of the stepped horn can be calculated analytically by assuming the length of its both sections equal to a quarter of the ultrasonic wavelength of the material. The calculated length of the stepped horn is 91 mm. The profiles of the catenoidal and stepped horns are also shown in Fig. 6(a).

Fig. 6(b) is a plot of the normalized displacements along the normalized length of the horns based on finite element computations. The displacements are normalized by the displacement at the back end of the horns. Therefore, the normalized displacement at the normalized length of 1 represents the displacement amplification. The stepped horn has the largest displacement amplification among the three types of the horns. The displacement amplification of the Bézier horn is nearly twice of that of the catenoidal horn. Fig. 7 shows the Mises stress along the normalized length of the horns based on the finite element computations. For the stepped horn, high stress occurs near the abruptly changing section. Stress concentration of the Bézier horn is significantly less than the other two types of horns. The lower Mises stress of the proposed horn can be attributed to its bell-shaped profile. The values of the displacement amplification M and maximum Mises stress $\sigma_{\max}$ of the three types of the horns are listed in Table 1. Although the stepped horn gives the highest displacement amplification, its high stress concentration at the step discontinuity makes it prone to failure.

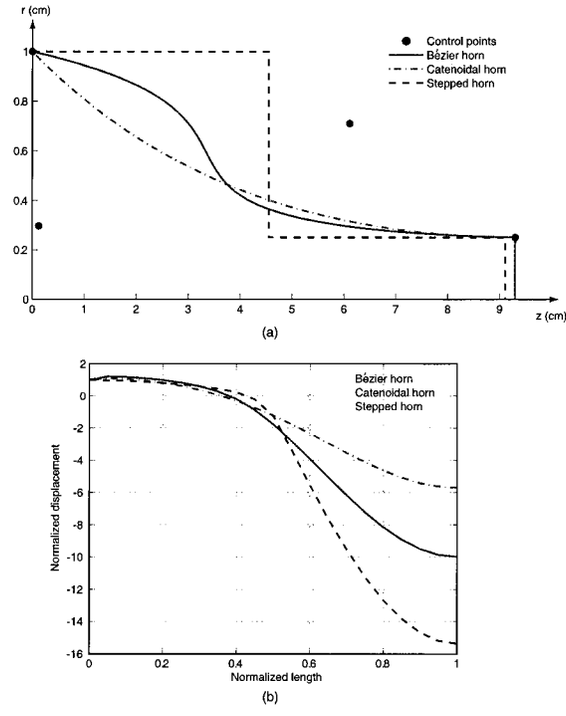

Fig. 6. (a) Profiles of the Bézier, catenoidal and stepped horns. The control points of the Bézier horn are also shown. (b) Normalized displacements along the normalized length of the horns.

Table 1. Comparison of the three types of the horns

	R_1^2 / R_2^2	*Length (mm)*	M	$\sigma_{\max}$ *(MPa)*
Catenoidal	4	93	5.9	76.5
Stepped	4	91	15.7	497
Bézier	4	93	10.5	32.4

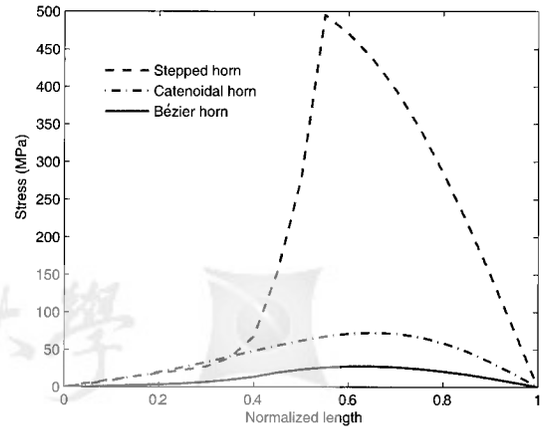

Fig. 7. Mises stress along the normalized length of the Bézier, catenoidal and stepped horns

4. FABRICATION, XPERIMENTS, AND DISCUSSIONS

In order to verify the effectiveness of the proposed horn, prototypes of a Bézier horn and a catenoidal horn are fabricated by a numerical control machining from a stainless steel. Dimensions of the prototypes are based on the finite element analyses. Fig. 8 is a photo of the fabricated horns. The horns are driven by the Langevin transducer. Fig. 9 is a schematic of the experimental apparatus for measurement of the displacement/vibration of the horns. The horns are mounted on an optical table. AC voltages are applied to the Langevin transducer by an electronic circuit that works like a nearly ideal voltage source. The vibration amplitude of the horns is measured by a fiber optic displacement/vibration sensor (MTI-2000, MTI Instruments Inc., US). The sensor probe is held by a micro manipulator. The measurement is recorded and analyzed by a data acquisition unit (PCI-5114, National Instruments Co., US).

Fig. 10 shows the measured vibration amplitude of the Bézier horn and the catenoidal horn as functions of the applied voltage at 27.9 kHz and 28.3 kHz, respectively. Three measurements are taken for each driving voltage. The vibration amplitudes of both horns increase as the driving voltage increases. The average displacement of the Bézier horn is approximately 50% greater than that of the catenoidal horn for the driving voltages considered. The simulation results listed in Table 1 shows that the Bézier horn has the displacement amplification 78% larger than the catenoidal horn while the experiment shows a nearly 50% of improvement. This discrepancy may come from the fact that a thread section is added to the horns as the connection part to the Langevin transducer and that has not been taken into account in the analyses. The manufacturing error and the misalignment due to assembly process may also contribute to the discrepancy.

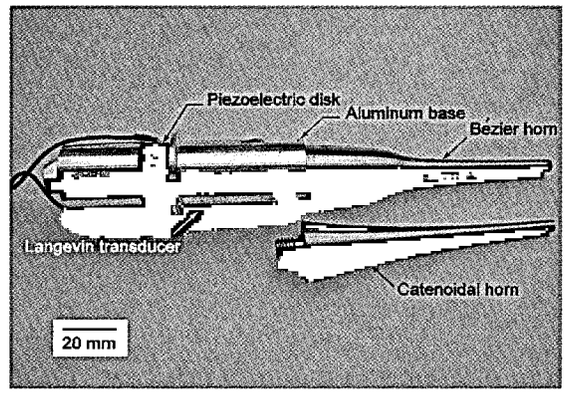

Fig. 8. Fabricated prototypes of the Bézier, and catenoidal horns. A Langevin transducer is also shown.

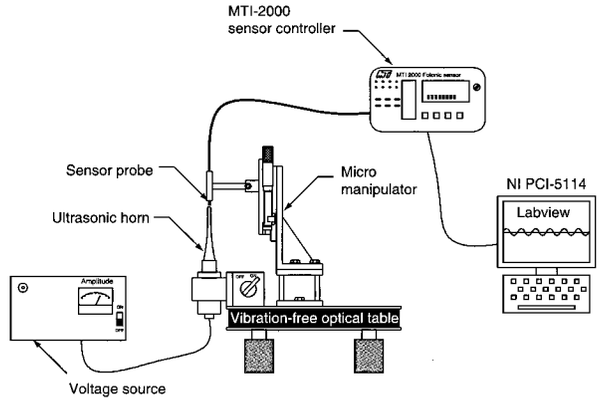

Fig. 9. Schematic of the experimental apparatus.

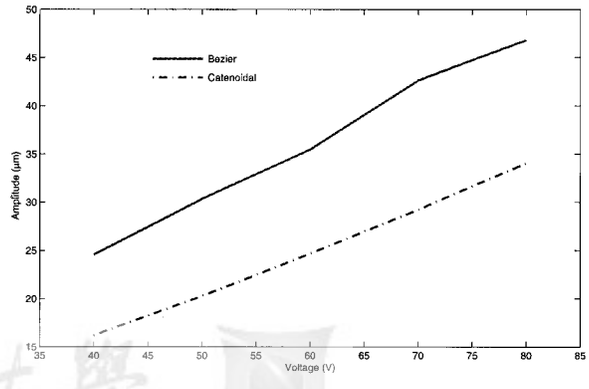

Fig. 10. Measured vibration amplitude of the Bézier and catenoidal horns as functions of the driving

5. CONCLUSIONS

A new horn with high displacement amplification is proposed. The profile of the horn is a cubic Bézier curve. Its design procedure is based on a multiobjective optimization algorithm and finite element analyses. Based on the finite element analyses, maximum Mises stress of the proposed horn is much lower than that of the catenoidal horn. Prototypes of the horn have been fabricated and tested. Experimental comparison of the working frequency between the designed and fabricated Bézier horns validates the effectiveness of the optimization design method. The displacement amplification of the proposed horn is 50% higher than that of the traditional catenoidal horn with the same length and end surface diameters.

ACKNOWLEDGEMENT

This work was financially supported by Precision Machinery Research and Development Center (Contract Number: 98TR10). Partial support of this work by a grant from National Science Council, Taiwan (Grant Number: NSC 96-2221-E-005-095) is greatly appreciated. The authors would like to express their appreciation to the National Center for High-Performance Computing (NCHC), Taiwan for their assistance. Helpful discussions with Mr. Yao-Tang Lin of Precision Machinery Research and Development Center are greatly appreciated.

REFERENCES

1. Perron, R.R., "The design and application of a reliable ultrasonic atomizer," *IEEE Transactions on Sonics and Ultrasonics*, Vol. SU-14, pp. 149-153 (1967).
2. Charles, S., Williams, R. and Poteat, T.L., "Micromachined structures in ophthalmic microsurgery," *Sensors and Actuators*, Vol. A21-A23, pp. 263-266 (1990).
3. Parrini, L., "Design of advanced ultrasonic transducers for welding devices," *IEEE Transactions on Ultrasonics, Ferroelectrics and Frequency Control*, Vol. 48, pp. 1632-1639 (2001).
4. Or, S.W., Chan, H.L.W., Lo, V.C. and Yuen, C.W., "Dynamics of an ultrasonic transducer used for wire bonding," *IEEE Transactions on Ultrasonics, Ferroelectrics and Frequency Control*, Vol. 45, pp. 1453-1460 (1998).
5. Parrini, L., "New technology for the design of advanced ultrasonic transducers for high-power applications," *Ultrasonics*, Vol. 41, pp. 261-269 (2003).
6. Hu, J., Nakamura, K. and Ueha, S., "An analysis of a noncontact ultrasonic motor with an ultrasonically levitated rotor," *Ultrasonics*, Vol. 35, pp. 459-467 (1997).
7. Iula, A., Caliano, G., Caronti, A. and M. Pappalardo, "A power transducer system for the ultrasonic lubrication of the continuous steel casting," *IEEE Transactions on Evolutionary Computation*, Vol. 50, pp. 1501-1508 (2003).
8. Iula, A., Pallini, S., Fabrizi, F., Carotenuto, R., Lamberti, N. and Pappalardo, M., "A high frequency ultrasonic bistoury designed to reduce friction trauma in cystectomy operations," in: Proceedings of 2001 IEEE Ultrasonics Symposium, pp. 1331-1334 (2001).
9. Lee, C.H. and Lal, A., "Silicon ultrasonic horns for thin film accelerated stress testing," in: Proceedings of 2001 IEEE Ultrasonics Symposium, pp. 867-870 (2001).
10. Eisner, E., "Design of sonic amplitude transformers for high magnification," *The Journal of the Acoustical Society of America*, Vol. 35, pp. 1367-1377 (1963).
11. Bangviwat, A., Ponnekanti, H.K. and Finch, R.D., "Optimizing the performance of piezoelectric drivers that use stepped horns," *The Journal of the Acoustical Society of America*, Vol. 90, pp. 1223-1229 (1991).

12. Sindayihebura, D. and Bolle, L., "Theoretical and experimental study of transducers aimed at low-frequency ultrasonic atomization of liquids," *The Journal of the Acoustical Society of America*, Vol. 103, pp. 1442-1448 (1998).
13. Nagarkar, B.N. and Finch, R.D., "Sinusoidal horns," *The Journal of the Acoustical Society of America*, Vol. 50, pp. 23-31 (1971).
14. Graff, K.F., *Wave motion in elastic solids*, Oxford : The Clarendon Press (1975).
15. Granet, C., James, G.L., Bolton, R. and Moorey, G., "A smooth-walled spline-profile horn as an alternative to the corrugated horn for wide band millimeter-wave applications," *IEEE Transactions on Antennas and Propagation*, Vol. 52, pp. 848-854 (2004).
16. Salmon, V., "A new family of horns," *The Journal of the Acoustical Society of America*, Vol.
17. pp. 212-218 (1946).17. Sherrit, S., Askins, S.A., Gradziol, M., Dolgin, B.P., Bao, X., Chang, Z. and Bar-Cohen, Y., "Novel horn designs for ultrasonic/sonic cleaning welding, soldering, cutting and drilling," in: Proceedings of the SPIE Smart Structures Conference 2002, Vol. 4701, Paper No. 34, San Diego, CA (2002).
18. Iula, A., Parenti, L., Fabrizi, F. and Pappalardo, M., "A high displacement ultrasonic actuator based on a flexural mechanical amplifier," *Sensors and Actuators A*, Vol. 125, pp. 118-123 (2006).
19. Abramov, O.V., "*High-intensity ultrasonics : theory and industrial applications*," Gordon and Breach Science Publishers, The Netherlands (1998).
20. Rogers, D. F. and Adams, J. A., "*Mathematical elements for computer graphics*," 2nd edition, McGRAW-Hill, New York (1990).
21. Woo, J., Roh, Y., Kang, K. and Lee, S., "Design and construction of an acoustic horn for high power ultrasonic transducers," in: Proceedings of 2006 IEEE Ultrasonics Symposium, pp. 1922-1925 (2006).
22. Fu, B., Hemsel, T. and Wallaschek, J., "Piezoelectric transducer design via multiobjective optimization," *Ultrasonics*, Vol. 44, pp. e747-e752 (2006).
23. Deb, K., Pratap, A., Agarwal, S. and Meyarivan, T., "A fast and elitist multiobjective genetic algorithm: NSGA-II," *IEEE Transactions on Evolutionary Computation*, Vol. 6, pp. 182-197 (2002).
24. Goldberg, D.E., "*Genetic algorithms in search, optimization & machine learning*," Addison Wesley Publishing Company, Inc., MA (1989).

Manuscript Received : Oct. 12, 2009
Revision Received : Nov. 02, 2009
and Accepted : Nov. 05, 2009